Physical Model of Deposition of Magnetic Particles in Lung Alveolus

[1]A. Krafčík, [2]P. Babinec, [1]I. Frollo

[1]Institute of Measurement Science, SAS, Bratislava, Slovakia
[2]Faculty of Mathematics, Physics and Informatics, UK, Bratislava, Slovakia
Email: andrej.krafcik@savba.sk

Abstract. *Due to lung anatomy, ability to use safely bigger particles for targeting, and reduced viscosity of air in comparison to blood, lungs represent unique opportunity for magnetic drug targeting. The most important issue is to understand dynamics of magnetic particle motion on alveolar level. Therefore we have developed physical model describing magnetic particle dynamics in a rhythmically expanding and contracting distal and proximal alveolus subjected to high-gradient magnetic field generated by cylindrical Halbach array of permanent magnets. We concluded that magnetic deposition can overcome both, aerodynamic forces as well as gravitational sedimentation.*

Keywords: Alveolus, Magnetic Targeting and Deposition, SPIONs, FEM, Halbach Array

1. Introduction

For the prediction of particle transport and deposition, and for the development of effective drug delivery strategies for the lung, it is the most important to understand flow phenomena on the alveolar level [1, 2]. Recently, it was pointed to using magnetic particles and gradient magnetic fields for targeting drugs in lungs of mice [3]. To further improve drug efficacy in the lungs, it may be advantageous to control aerosol deposition and to target aerosols using magnetic gradient fields. Our aim was therefore to develop physical model describing magnetic deposition of particles in lung alveolus [4].

2. Physical Model

The differential equation governing the motion of a spherical particle with mass m_p and nonzero magnetic moment $\boldsymbol{\mu}_p$ subjected to gravity field $\mathbf{g}$ and external magnetic field $\mathbf{B}$ is

$$m_p \frac{\mathrm{d}^2\mathbf{r}_p}{\mathrm{d}t^2} = \mathbf{F}_D + m_p\mathbf{g} + \left(\boldsymbol{\mu}_p \cdot \nabla\right)\mathbf{B}, \qquad (1)$$

where $\mathbf{r}_p$ is the instantaneous particle position, and $\mathbf{F}_D$ is the drag force exerted on the particle, with neglected stochastic Brownian forces. For details see our paper [4].

Drag Force and Alveolar Flow Model

The drag force exerted on a spherical particle with D_p in diameter (and with slip correction factor C) suspended in Stokesian flow field $\mathbf{v}_f$ of air with dynamic viscosity η_f is given as

$$\mathbf{F}_D = 3\pi\eta_f D_p \left(\mathbf{v}_f - \mathbf{v}_p\right)/C. \qquad (2)$$

Alveolar Flow Model (AFM) [1]

AFM views single-alveolus configuration as a hemispherical cavity attached at a rim to a flat plane. The flow passing through the alveolar duct near the alveolus is approximated by a simple oscillatory shear flow over the flat plane, far upstream or downstream from the hemispherical cavity. The plane and the attached cavity perform an oscillatory, self-similar expansion and contraction movement. Assuming that the flow field is governed by the creeping flow equations, superposition of the following two flow fields is allowed: 1) *expansion flow* (alveolar flow)—the flow induced by the self-similar expansion and contraction of the alveolus with zero downstream flow inside the adjacent airways, and 2) *shear flow* (ductal flow)–the flow induced by shear flow over a hemispherical rigid cavity with vanishing velocity at the boundaries. Due to the quasi-steadiness of Stokes flows, the time variable can be viewed as a parameter that enters the problem via time dependent boundary conditions.

Expansion Flow

Expansion flow velocity vector field $\mathbf{v}^{\mathrm{H}}$ induced by a unit surface radial velocity for a unit radius hemisphere [1] in polar toroidal coordinate system (ξ,η,ϕ):

$$\begin{aligned} v^{\mathrm{H}}{}_{\xi} &= -\frac{\sinh\xi\left(\cosh\xi\cos\eta - 2\sin^2\eta - 1\right)}{\left(\cosh\xi-\cos\eta\right)^2} - \frac{3}{2}\sin\eta\tanh\frac{\xi}{2}\left(\frac{1-\cos\eta}{\cosh\xi-\cos\eta}\right)^{1/2} \\ &+ \frac{3}{2}\frac{\sin\eta\sinh\xi}{\left(\cosh\xi-\cos\eta\right)^{1/2}}\int_0^\infty F_h(\alpha,\eta)P'_{-1/2+\mathrm{i}\alpha}(\cosh\xi)\,\mathrm{d}\alpha \\ &- \sinh\xi\left(\cosh\xi-\cos\eta\right)^{1/2}\int_0^\infty \frac{\partial F_h(\alpha,\eta)}{\partial\eta}P'_{-1/2+\mathrm{i}\alpha}(\cosh\xi)\,\mathrm{d}\alpha, \\ v^{\mathrm{H}}{}_{\eta} &= +\frac{\sin\eta\left(-\cosh^2\xi - 2\cos\eta\cosh\xi + 3\right)}{\left(\cosh\xi-\cos\eta\right)^2} - \frac{3}{2}\frac{\left(1-\cos\eta\right)^{3/2}}{\left(\cosh\xi-\cos\eta\right)^{1/2}} \\ &+ \frac{\left(\cosh^2\xi - \cosh\xi\cos\eta + 3\right)}{2\left(\cosh\xi-\cos\eta\right)^{1/2}}\int_0^\infty F_h(\alpha,\eta)P'_{-1/2+\mathrm{i}\alpha}(\cosh\xi)\,\mathrm{d}\alpha \\ &+ \sinh^2\xi\left(\cosh\xi-\cos\eta\right)^{1/2}\int_0^\infty F_h(\alpha,\eta)P''_{-1/2+\mathrm{i}\alpha}(\cosh\xi)\,\mathrm{d}\alpha, \end{aligned} \tag{3}$$

where: $P'_{-1/2+\mathrm{i}\alpha}(s)$ and $P''_{-1/2+\mathrm{i}\alpha}(s)$ are the derivatives of the Legendre function of complex degree, and $F_h(\alpha,\eta)$ is the representation function for hemispherical alveolus [1, 4].

Shear Flow

Shear flow velocity vector field $\mathbf{v}^{\mathrm{P}}$ induced by a unit shear flow over a unit hemispherical cavity was studied in [2], employing a numerical boundary integral method. The velocity field depends on the three independent unknown functions of the coordinates (ρ,z) to be determined numerically. The solution possesses the general following form in Cartesian coordinates

$$\mathbf{v}^{\mathrm{P}} = \left[v^{\mathrm{P}}{}_1(\rho,z)\cos^2\phi + v^{\mathrm{P}}{}_2(\rho,z),\, v^{\mathrm{P}}{}_1(\rho,z)\cos\phi\sin\phi,\, v^{\mathrm{P}}{}_3(\rho,z)\cos\phi\right]^T. \tag{4}$$

The 3D solution for $\mathbf{v}^{\mathrm{H}}$ and $\mathbf{v}^{\mathrm{P}}$ obtained in [1] and [2], defined for unit depression radius and unit shear rate, can be utilize to solve the quasi-steady problem for alternating shear rates embedded in time protocols, and yields for drag force:

$$\mathbf{F}_D = -\frac{3\pi\eta_f D_p}{C}\left\{R_0\beta\omega\left[\sin(\omega t)\mathbf{v}^{\mathrm{H}}\left(\frac{\mathbf{r}_p}{R(t)}\right) + \gamma\sin(\omega t+\delta)\mathbf{v}^{\mathrm{P}}\left(\frac{\mathbf{r}_p}{R(t)}\right)\right] + \frac{\mathrm{d}\mathbf{r}_p}{\mathrm{d}t}\right\}, \tag{5}$$

where ω is the breathing frequency, R_0 is the mean radius of the alveolus, $R_0\beta$ is the alveolus expansion amplitude, δ is phase difference between expansion and shear flow, and γ is a ratio of their amplitudes ($\gamma > 1000$ at the first few generations (e.g. 16–19th), and remains $\gamma > 100$ for the most of the acinar generations).

Magnetic Force and FEM Model of Magnetic Field Source

Magnetic Force for fully magnetically saturated particle with magnetic moment $|\boldsymbol{\mu}_p|$ (for values of parameters see Table 1) in external magnetic field $\mathbf{B}$ is

$$\mathbf{F}_M = |\boldsymbol{\mu}_p|((\mathbf{B}/B)\cdot\nabla)\mathbf{B}\,. \tag{6}$$

As source has been used cylindrical Halbach array of permanent magnets (for finite element method (FEM) model see Fig. 1) [4]. Gradient of magnetic field, $\mathbf{G}_M = ((\mathbf{B}/B)\cdot\nabla)\mathbf{B}$, has reached value almost $G_M \approx 100$ T/m at alveolus location.

Table 1. Parameters of particles used in simulations [4].

Quantity	Magnetite sphere	Droplet with SPIONs[a]
diameter, D_p (m)	1.0×10^{-6}	3.5×10^{-6}
mass, m_p (kg)	2.6×10^{-15}	22.9×10^{-15}
magnetic moment[b], $\lvert\boldsymbol{\mu}_p\rvert$ ($A\cdot m^2$)	250×10^{-15}	26.4×10^{-15}

[a] Water aerosol droplet with content of 2930 superparamagnetic iron-oxid nanoparticles (SPIONs) [3].

[b] Magnetic moment of fully magnetically saturated particle.

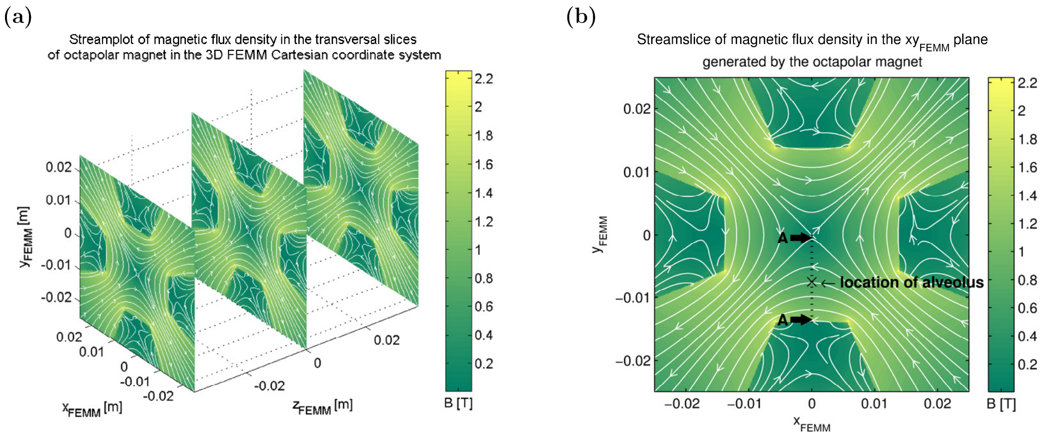

Fig. 1. FEM model of cylindrical Halbach array as a source of gradient magnetic field. Obtained using FEMM v.4.2 (D. Meeker). [4]

3. Results

Simulations have been performed using MATLAB built in ode15s ordinary differential equations solver for alveolus with the following geometrical and physiological properties: $R_0 = 150\,\mu\text{m}$, $\beta = 0.1$, $\gamma = 300$ (distal airways generations), $\delta = 0°$, and $\omega = 12$ breaths-per-minute; see Fig. 2. Also, in similar way for $\gamma = 1000$ (proximal airways generations).

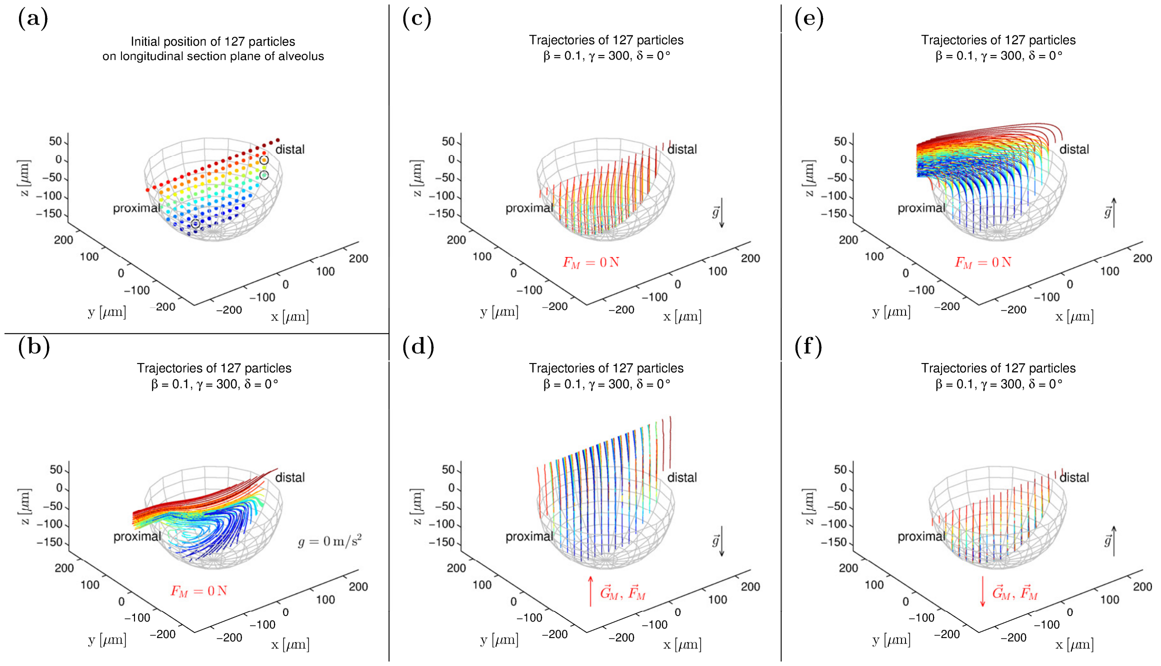

Fig. 2. Simulation results [4]: (a) initial positions; and trajectories of droplets with SPIONs in alveolus: (b) in gravity-free and magnetic-free conditions, (c, e) with presence of gravity and magnetic-free conditions, and (d, f) with presence of gravity and magnetic gradient.

4. Conclusions

Magnetic deposition of particles in alveolus can overcome both, aerodynamic forces and gravitational sedimentation, not only in the case of magnetite spheres with large magnetic moment, but also in the case of water aerosol droplets with content of SPIONs, whose magnetic moment is reduced in comparison with magnetite spheres. It was occurred not only in alveolus in distal airways generations with reduced ductal flows, but also in proximal ones.

Acknowledgements

This work was supported by Grant Agency of the Slovak Academy of Sciences (VEGA 2/0013/14 and VEGA 1/0871/14); and realized on MATLAB ISS CVTI SR.

References

[1] Haber S, Butler JP, Brenner H, Emanuel I, Tsuda A. Shear flow over a self-similar expanding pulmonary alveolus during rhythmical breathing. *Journal of Fluid Mechanics*, 405:243-268, 2000.

[2] Pozrikidis C. Shear flow over a plane wall with an axisymmetric cavity or a circular orifice of finite thickness. *Physics of Fluids*, 6(1):68-79, 1994.

[3] Dames P, Gleich B, Flemmer A, Hajek K, Seidl N, Wiekhorst F, Eberbeck D, Bittmann I, Bergemann C, Weyh T, Trahms L, Rosenecker J, Rudolph C. Targeted delivery of magnetic aerosol droplets to the lung. *Nature Nanotechnology*, 2(8):495-499, 2007.

[4] Krafcik A, Babinec P, Frollo I. Computational analysis of magnetic field induced deposition of magnetic particles in lung alveolus in comparison to deposition produced with viscous drag and gravitational force. *Journal of Magnetism and Magnetic Materials*, 380:46-53, 2015.